Assessing common density functional approximations for the *ab initio* description of monovacancies in metals

L. Delczeg,[1] E. K. Delczeg-Czirjak,[1] B. Johansson,[1,2] and L. Vitos[1,2,3]

[1]*Applied Materials Physics, Department of Materials Science and Engineering, Royal Institute of Technology, SE-10044 Stockholm, Sweden*

[2]*Division for Materials Theory, Department of Physics and Materials Science, Uppsala University, SE-75121 Uppsala, Sweden*

[3]*Research Institute for Solid State Physics and Optics, P.O. Box 49, H-1525 Budapest, Hungary*

Using the exact muffin-tin orbitals method, we investigate the accuracy of five common density functional approximations for the theoretical description of the formation energy of monovacancies in three close-packed metals. Besides the local density approximation (LDA), we consider two generalized gradient approximation developed by Perdew and co-workers (PBE and PBEsol) and two gradient-level functionals obtained within the subsystem functional approach (AM05 and LAG). As test cases, we select aluminum, nickel, and copper, all of them adopting the face centered cubic crystallographic structure. Our results show that, compared to the recommended experimental values, LDA is be the most reliable approximation for the vacancy formation energies in these metals. However, taking into account also the performances of the functionals for the equation of state changes the final verdict in favor of the generalized gradient approximations.

PACS number(s): 71.15.Mb, 71.15.Nc, 61.72.jd, 68.47.De

I. INTRODUCTION

Point defects are important for the thermophysical and mechanical properties of solids. They include substitutional and interstitial impurities, self interstitials and vacancies. Vacancies are common defects at high temperature and also in irradiated materials, and play a key role for the kinetic properties, such as diffusion. Today, reliable experimental data for the formation energy of monovacancies exist for most of the metals and intermetallic compounds.

The theoretical description of the formation energy of monovacancies has always been a benchmark for the approximations of the exchange-correlation density functionals.[1] Vacancies in metals involve both slowly and rapidly varying density regimes. The prior corresponds to the oscillating metallic density around the vacancy and the latter to the electronic surface near the core of the vacancy. Because of that, vacancies represent a critical test case for functionals going beyond the local density approximation (LDA).[2] The LDA functional describes accurately the nearly homogeneous electron gas, but is expected to break down in systems with rapid density variations. To incorporate effects due to inhomogeneous electron density, researchers made use of the density gradient expansion of the exchange-correlation functional[2] and arrived to the so-called generalized gradient approximation (GGA). Nowadays, the most commonly accepted GGA for solids is the PBE functional proposed by Perdew, Burke, and Ernzerhof.[3] Recently, Perdew and co-workers[4] introduced a revised Perdew, Burke, and Ernzerhof (PBE) functional, referred to as PBEsol. The PBEsol functional is a redesigned PBE with the aim to yield accurate equilibrium properties of densely packed solids and remedy the deficiencies of the former GGA functionals for surfaces. Simultaneously to GGA, a different concept for improving the density functional approximations was put forward by Kohn and Mattsson.[5] The proposed model was first elaborated by Vitos and co-workers[6,7] and later further developed by Armiento and Mattsson[8] within the subsystem functional (SSF) approach.[9] The corresponding approximations are referred to as the Local Airy Gas Approximation (LAG) (Ref. 6) and the AM05 functional.[9] Both functionals from the SSF family as well as the PBEsol functional from the GGA family include important surface effects and, therefore, are supposed to perform well for systems with electronic surface.

A number of theoretical studies focused on the *ab initio* determination of the formation energies and crystal structure of vacancies in metals.[8,10–16] Most of these investigations employed density functional theory based on LDA or gradient-level approximations from the GGA or SSF families. Nevertheless, none of the former studies considered the recently developed PBEsol functional and made a systematic assessment of its performance for the vacancy formation energies and compared it to other common approximations. The accuracy of PBEsol was recently tested for metallic bulk[17,18] and surface systems.[17] It was found that, on average, PBEsol gives equilibrium volumes and bulk moduli in close agreement with PBE, LAG, and AM05, whereas for close-packed metal surfaces, PBEsol has the same performance as AM05, giving significantly larger and presumably more accurate surface energies than PBE and LAG.

Our aim is to investigate the accuracy of the PBEsol approximation for vacancy formation energies in metals. To this end, we have performed a series of *ab initio* calculations using the LDA, PBE, PBEsol, AM05, and LAG approximations. In this test, we have considered three close-packed metals: Al, Ni, and Cu; all of them having the face centered cubic (fcc) crystallographic lattice. Numerous former theoretical studies concentrated on fcc Al, providing accurate theoretical vacancy formation energies at different density functional approximation levels. Nickel and copper have been selected as two representative fcc nonmagnetic (Cu) and magnetic (Ni) transition metals. To our knowledge, the vacancies in Cu and Ni have been studied only at LDA and PBE levels.

The structure of the paper is as follows. The theoretical tool is presented in Sec. II, where we also give the most important details of the numerical calculations. The results are presented and discussed in Sec. III Here, we start by establishing the accuracy of the present computational method by making use of the former theoretical vacancy formation energies obtained within LDA, PBE, and AM05. In the second part of this section, we assess the PBEsol approximation by comparing the present theoretical results with the available experimental data and then discuss the relative merits of the five approximations.

II. COMPUTATIONAL METHOD

A. Total energy calculations

All calculations have been carried out using density functional theory[1,2] formulated within the exact muffin-tin orbitals (EMTO) method[19–22] in combinations with supercell technique. The EMTO method is an improved screened Korringa-Kohn-Rostoker method, where the one-electron potential is represented by large overlapping muffin-tin potential spheres. By using overlapping spheres, one describes more accurately the crystal potential, when compared to the conventional non overlapping muffin-tin approach.[22,23] The EMTO method, in combination with the full charge density technique,[24] has been applied successfully in the theoretical study of the thermophysical properties of metallic alloys[21,22,25–35] and complex oxides.[36–39]

In the self-consistent calculations, the exchange-correlation term was described within the local density approximation. Here, we adopted the Perdew and Wang parametrization[40] of the quantum Monte Carlo data by Ceperley and Alder.[41] The gradient terms in the PBE, PBEsol, AM05, and LAG approximations were included within a perturbative approach.[42] Namely, we used the total charge density obtained within LDA to compute the gradient-level total energies. This approach suits very well the full charge density formalism[24] and has been shown to produce errors in the equation of state that are within the numerical accuracy of our calculations.[17] The accuracy of the perturbative approach for the vacancy formation energy will be established in Sec. III A.

B. Vacancy formation energy

We started our investigation by establishing the equation of state of fcc Al, Ni and Cu. The bulk total energy was calculated for seven different volumes around the experimental equilibrium volume and the theoretical equilibrium Wigner-Seitz radius (w_0), bulk total energy (E_0), and bulk modulus (B_0) were extracted from a Morse type of function[43] fitted to the calculated total energies.

For calculating the vacancy formation energy, we used supercells built up from the conventional fcc unit cell. Previously, the effect of the size of the supercell on the vacancy formation energy was thoroughly examined for several fcc metals.[10,11,21] It was found that, as long as the proper convergence of the Brillouin zone sampling is ensured, relatively small supercells are already enough for an accurate descrip-

tion of the vacancy formation energies. Because of that, here we adopted a $2 \times 2 \times 2$ supercell with simple cubic (sc) symmetry and a $2 \times 2 \times 2$ supercell with body centered cubic (bcc) symmetry. As the primitive cells of the sc and bcc supercells contain 32 and 16 sites, we denote them by sc32 and sc16, respectively. One of the 32 (16) sites was substituted by vacancy corresponding to 1/32 (1/16) vacancy concentration in bulk metal.

To obtain the unrelaxed vacancy formation energy $[E_v(0)]$ at zero pressure, first we calculated the equilibrium Wigner-Seitz radius (w_{SC}) and the total energy $[E_{SC}(0)]$ of the 32 and 16-site supercells with fixed underlying lattice. Then the volume-relaxed vacancy formation energy was obtained as $E_v^N(0) = E_{SC}(0) - (N-1)E_0$, where N stands for 16 or 32. Experiments show that the crystal structure is distorted around the vacancy. For a more realistic geometry around the vacancy, in the present study we included the local lattice relaxation by computing the total energy for the supercell $[E_{SC}(\eta)]$ as a function of the distance $d = (1+\eta)d_0$ between the vacancy and the 12 atoms from the first coordination shell around the vacancy. Here, d_0 is the ideal unrelaxed nearest neighbor distance in the fcc lattice. Taking into account the lattice relaxation beyond the first coordination shell has been found to have a small effect on the vacancy formation energy.[13] The final vacancy formation energy (E_v) and the equilibrium local relaxation (η_0) around the vacancy were obtained from the minimum of the formation energy $E_v^N(\eta) = E_{SC}(\eta) - (N-1)E_0$, viz., $E_v^N = \min_\eta E_v^N(\eta) = E_v^N(\eta_0)$.

C. Numerical details

The EMTO basis set included s, p, and d orbitals for Al and s, p, d, and f orbitals for Ni and Cu. The one-electron equations were solved within the scalar-relativistic approximation. The Al-$3s^2 3p^1$, Ni-$3d^8 4s^2$, and Cu-$3d^{10} 4s^1$ states were considered as valence states and the core states were recalculated after each iteration. Aluminum and copper were treated as nonmagnetic metals, whereas nickel was described in the ferromagnetic phase. For each element and crystal lattice, the EMTO Green function was calculated self-consistently for 16 complex energy points distributed exponentially on a semicircular contour, which included states within 1 Ry below the Fermi level. In the one-center expansion of the full charge density, we adopted an l-cutoff of 10. All potential spheres were set at the corresponding Wigner-Seitz spheres. For the local lattice relaxation around the vacancy, we used both compressed ($\eta = -6, -4, -2\%$) and expanded ($\eta = 2, 4, 6\%$) nearest neighbor distances. The minimum of $E_v(\eta)$ was obtained from a second order polynomial fit. The k-space sampling was performed with a uniform k mesh within the Brillouin zone. The actual number of inequivalent k points was established (see Sec. III A) so that the numerical error of the vacancy formation energy to be below 0.01 eV.

III. RESULTS

A. Establishing the numerical accuracy

One of the fundamental questions in all electronic structure calculation for solids is the Brillouin zone sampling. It

TABLE I. Total energy convergence for bulk fcc Al as a function of the number of k points in the irreducible Brillouin zone. The energy differences (in meV) are shown for all five exchange-correlation approximations considered here and they are given relative to the those obtained for the largest number of k points.

# k points	LDA	PBE	PBEsol	AM5	LAG
505	1.306	1.483	1.320	1.374	1.415
916	0.585	0.381	0.449	0.395	0.558
2304	0.136	0.109	0.218	0.282	0.041
6281	0.000	0.000	0.000	0.000	0.000

has been shown that, without a proper k-mesh convergence, no accurate vacancy formation energies can be computed.[11] Since it is known that the k-point convergence of the total energy of transition metals is superior compared to the simple metals, the present convergence test was performed only for fcc Al.

In Table I, we show the total energies of bulk fcc Al for the five different exchange-correlation approximations as a function of the number of k points in the irreducible part of the Brillouin zone (IBZ). As expected, the k-point convergence is rather independent of the exchange-correlation approximation. Moreover, we find that 2304 k points in the IBZ ensures a convergence better than 0.3 meV for the total energy per atom. For the largest system considered here, this results in 9.6 meV error in the total energy per 32 atoms, which is in line with our target numerical error bar of 0.01 eV for the vacancy formation energy. Therefore, all our bulk calculations for Al, Ni, and Cu were performed by using 2304 uniformly distributed k points in the IBZ of the fcc structure.

Next, using the 2304 k mesh, we computed the equilibrium volume and equilibrium total energy of fcc Al, Cu, and Ni. The bulk total energy (E_0) can be determined by fitting the total energies computed as a function of the Wigner-Seitz radius $[E(w)]$ using an equation of state and finding the minimum of the fit function. Alternatively, the equilibrium total energy (E_0') can also be obtained by repeating the calculation at the equilibrium radius w_0 obtained from the minimum of the fit function. The difference between the two energies ($\Delta^1 \equiv |E_0' - E_0|$) may be interpreted as the numerical error associated with the total energy calculation. Repeating the above procedure for the two supercells filled up with atoms (without vacancy), we obtain the corresponding errors Δ^{16} and Δ^{32}. In these supercell calculations, we used 165 and 140 k points within the irreducible part of the sc and bcc Brillouin zones, respectively. Obviously, with properly sampled Brillouin zones for the supercells, we should have $\Delta^{32} \approx 2\Delta^{16} \approx 32\Delta^1$. The present LDA-level errors for Al are $\Delta^1 = 0.3$ meV, $\Delta^{16} = 6.8$ meV, and $\Delta^{32} = 10.1$ meV. We note that the other four exchange-correlation functionals yield errors below those obtained with LDA. Based on the above figures, we conclude that our k-space integrations for the supercells are well converged. Furthermore, the numerical errors in the calculated total energies (including the errors from the fit for the equation of state) are consistent with the error bar of 0.01 eV set for the vacancy formation energy.

In order to assess the errors associated with the perturbative approach employed for the gradient-level exchange-correlation functionals, in addition to the LDA self-consistent calculations we also carried out a fully self-consistent PBE calculation for the vacancy formation energy of fcc Al using the sc16 supercell. The two PBE vacancy formation energies differ by somewhat less than 0.03 eV. Since PBE has the strongest gradient term among the gradient-level functionals considered here, we assume that the above deviation represents the upper limit for the error introduced by the perturbative approach. We conclude that the non-self-consistent treatment of the gradient-level functionals increases the error bar of the PBE, PBEsol, AM05, and LAG vacancy formation energies to 0.03 eV. This error corresponds approximately to 4%, 2%, and 3% of the experimental vacancy formation energy for Al, Ni, and Cu (see Sec. III C 2).

B. Equations of state for bulk Al, Ni, and Cu

The present equilibrium Wigner-Seitz radius (w_0) and bulk modulus (B_0) of fcc Al, Ni, and Cu are compared with former theoretical and experimental data in Table II. First, we compare our results with those obtained using the projector augmented wave,[45] linear combination of atomic orbitals,[18] and linear augmented plane wave[46] methods. In general, the agreement between the three sets of theoretical values is very good, indicating that EMTO accurately describes the equations of state of fcc Al, Ni, and Cu. The somewhat larger deviation for the bulk modulus could partly be ascribed to the fit functions employed in the calculations. Our bulk parameters were extracted from a Morse type of function,[43] whereas in former studies a less flexible Murnaghan fit[22,47] was adopted.

Compared to the experimental values[44] from Table II, we find that the average errors of the EMTO results obtained within LDA, PBE, PBEsol, AM05, and LAG are 15.2, 3.7, 10.4, 11.1, and 7.3%, respectively. Thus, PBE gives the best performance for the equations of state and LAG is placed on the second place. It is interesting that the PBEsol and AM05 approximations yield similar average errors. This observation is in line with a former assessment made on a significantly larger database (see Tables II and III from Ref. 17). Since the experimental data refers to room temperature and no phonon effects are included in the present theoretical values, it is not possible to resolve the small difference between the accuracies of PBEsol and AM05 for the equation of state of Al, Ni, and Cu.

TABLE II. Theoretical and experimental (Ref. 44) equilibrium Wigner-Seitz radius (w_0 in Bohr) and bulk modulus (B_0 in GPa) for fcc Al, Cu, and Ni. The present results, shown for five different exchange-correlation approximations, are compared to former theoretical data obtained using full-potential methods based on the projector augmented wave (Ref. 45), linear combination of atomic orbitals (Ref. 18), and linear augmented plane wave (Ref. 46) techniques.

System		LDA	PBE	PBEsol	AM05	LAG	Expt.
Al	w_0	2.95	2.99	2.97	2.96	2.98	2.991
		2.94[a], 2.94[b]	2.99[a], 2.98[b]	2.96[b]	2.96[a]		
	B_0	81.2	75.7	80.1	84.8	76.5	72.8
		81.4[a], 83.8[b]	75.2[a], 78.0[b]	82.6[b]	83.9[a]		
Ni	w_0	2.53	2.61	2.56	2.56	2.57	2.602
			2.60[a]				
	B_0	243	198	223	222	214	179
			199[c]				
Cu	w_0	2.60	2.69	2.64	2.64	2.65	2.669
		2.60[a], 2.60[b]	2.69[a], 2.68[b]	2.63[b]	2.63[a], 2.63[b]		
	B_0	182	142	165	163	155	133
		180[a], 190[b]	134[a], 142[b]	166[b]	157[b]		

[a]Reference 45.
[b]Reference 18.
[c]Reference 46.

C. Vacancy formation energy for Al, Ni, and Cu

1. Supercell and lattice relaxation

The volume-relaxed vacancy formation energies for fcc Al, Ni, and Cu $[E_v(\eta)]$ are shown in Table III as a function of η describing the local lattice relaxation around the vacancy. Results are displayed for supercells with 16 $[E_v^{16}(\eta)]$ and 32 $[E_v^{32}(\eta)]$ atoms and for the LDA, PBE, PBEsol, AM05, and LAG exchange-correlation approximations.

The minimum of $E_v(\eta)$ gives the vacancy formation energy E_v (shown in Table IV) and the equilibrium relaxation η_0. We find that η_0 exhibits a weak dependence on the exchange-correlation approximation. For instance, in the case of sc16 Al, for η_0 we get -1.370, -1.359, -1.363, -1.361, and -1.359 for LDA, PBE, PBEsol, AM05, and LAG, respectively. Similar behavior is seen for the sc32 supercell and for Ni and Cu as well. Figure 1 compares the LDA and PBE values for $E_v^{32}(\eta)$ for Al, Ni, and Cu. We

TABLE III. Vacancy formation energies (in eV) for fcc Al, Ni, and Cu as a function of the local lattice relaxation (η). Results are shown 16-atoms and 32-atoms supercells and for LDA, PBE, PBEsol, AM05, and LAG.

η (%)	LDA			PBE			PBEsol			AM05			LAG		
	Al	Ni	Cu	Al	Ni	Cu	Al	Ni	Cu	Al	Ni	Cu	Al	Ni	Cu
							sc16								
−6	3.02	4.64	3.46	2.83	4.02	2.89	3.04	4.47	3.30	3.23	4.56	3.37	2.85	4.24	3.07
−4	1.33	2.58	1.88	1.26	2.27	1.60	1.40	2.55	1.85	1.57	2.63	1.91	1.24	2.34	1.66
−2	0.64	1.70	1.23	0.62	1.51	1.06	0.74	1.73	1.25	0.89	1.80	1.31	0.58	1.54	1.08
0	0.85	1.91	1.41	0.81	1.65	1.18	0.94	1.89	1.40	1.09	1.98	1.47	0.77	1.71	1.22
2	1.91	3.13	2.36	1.79	2.64	1.93	1.96	3.00	2.26	2.13	3.11	2.34	1.78	2.80	2.06
							sc32								
−6	2.79	4.40	3.28	2.64	3.85	2.77	2.82	4.25	3.14	3.00	4.34	3.21	2.65	4.03	2.93
−4	1.34	2.54	1.84	1.28	2.24	1.57	1.42	2.50	1.81	1.58	2.58	1.88	1.26	2.31	1.63
−2	0.70	1.73	1.24	0.67	1.52	1.05	0.80	1.73	1.25	0.94	1.81	1.31	0.64	1.55	1.08
0	0.81	1.87	1.39	0.77	1.60	1.15	0.91	1.85	1.37	1.05	1.93	1.44	0.75	1.67	1.19
2	1.66	2.91	2.22	1.57	2.46	1.81	1.73	2.80	2.13	1.89	2.90	2.21	1.55	2.60	1.92

TABLE IV. Vacancy formation energies (in eV) for fcc Al, Ni, and Cu. Results are shown for 16-atoms and 32-atoms supercells and for the LDA, PBE, PBEsol, AM05, and LAG exchange-correlation approximations.

	LDA			PBE			PBEsol			AM05			LAG		
	Al	Ni	Cu	Al	Ni	Cu	Al	Ni	Cu	Al	Ni	Cu	Al	Ni	Cu
sc16	0.63	1.65	1.18	0.61	1.46	1.03	0.73	1.67	1.20	0.89	1.75	1.26	0.58	1.50	1.01
sc32	0.65	1.67	1.21	0.62	1.46	1.02	0.75	1.67	1.21	0.89	1.75	1.28	0.59	1.49	1.04

observe that the difference between the LDA and PBE curves is somewhat larger for large positive and negative distortions. However, in all three cases $\eta_0^{LDA} \approx \eta_0^{PBE}$. The element dependence of η_0 also turns out to be small. Within the numerical accuracy of our fitting ($\pm 0.05\%$), η_0 for Al, Ni, and Cu are identical: -1.4% for sc16 and -1.3% for sc32.

Table IV demonstrates the effect of the size of the supercell on E_v. In the case of Al, it is found that the vacancy formation energies increase by 0.00–0.02 eV, depending on the exchange-correlation approximation, when going from the 16-atoms supercell to the 32-atoms supercell. The size effects for Cu and Ni are similar to that for Al. The above finding confirms the previous observation about the size of the supercell and the proper Brillouin zone sampling.[10,11,21] In the following, we compare the present theoretical vacancy formation energies obtained for the 32-atoms supercell with former theoretical and experimental data.

2. Comparisons: Theory versus experiment

The fully relaxed vacancy formation energies for fcc Al, Ni and Cu are compared with the available theoretical and experimental data[48] in Tables V–VII. The theoretical description of the vacancies in Al has been used many times as a benchmark for the exchange-correlation approximations. Because of that, for this system theoretical vacancy formation energies are available within LDA, PBE, AM05, and LAG.[8,49] The deviation between the present E_v and those obtained using the full-potential Korringa-Kohn-Rostoker (FPKKR) method[49] (Table V) is within the numerical error of our calculations. Somewhat larger differences can be seen between our results and those calculated using a pseudopo-

tential (PP) approach.[8] These deviations may, however, be ascribed to the differences between the computational tools (all electron versus pseudopotential) and numerical details. Nevertheless, the trends predicted from EMTO and PP calculations when going from LDA to PBE, AM05, and LAG are in line with each other indicating the robustness of the theoretical data.

Comparing the EMTO results for Al with the recommended experimental value of 0.67 ± 0.03 eV,[50] for the relative deviations within LDA, PBE, PBEsol, AM05 and LAG we get 3.0, 9.0, 11.9, 32.8, and 11.9%, respectively. The surprisingly good LDA result was suggested to be coincidental.[8] Except AM05, which gives unexpectedly large E_v, the present gradient corrected functionals yield similar errors for the vacancy formation energy of fcc Al. It is important to point out that the main difference between LAG and AM05 is the correlation functional: the prior uses the LDA correlation by Perdew and Wang,[40,41] while the latter uses a correlation functional generated from the jellium surface data.[8] Obviously, this gradient-level correlation term is responsible for the 0.3 eV difference between AM05 and LAG results. Since the PBEsol correlation is also based on the jellium surface data,[4] it seems that the often quoted "error cancellation" between the exchange and correlation terms is more effective in PBEsol than in AM05.

For ferromagnetic fcc Ni (Table VI), the only available theoretical vacancy formation energy was obtained using the linear muffin-tin orbitals method (LMTO) in combination with LDA.[10] In spite of the fact that the reported LMTO value (1.78 eV) corresponds to a rigid fcc lattice (only volume-relaxed), it agrees well with the mean experimental value of 1.79 ± 0.05 eV.[50] The relative difference between
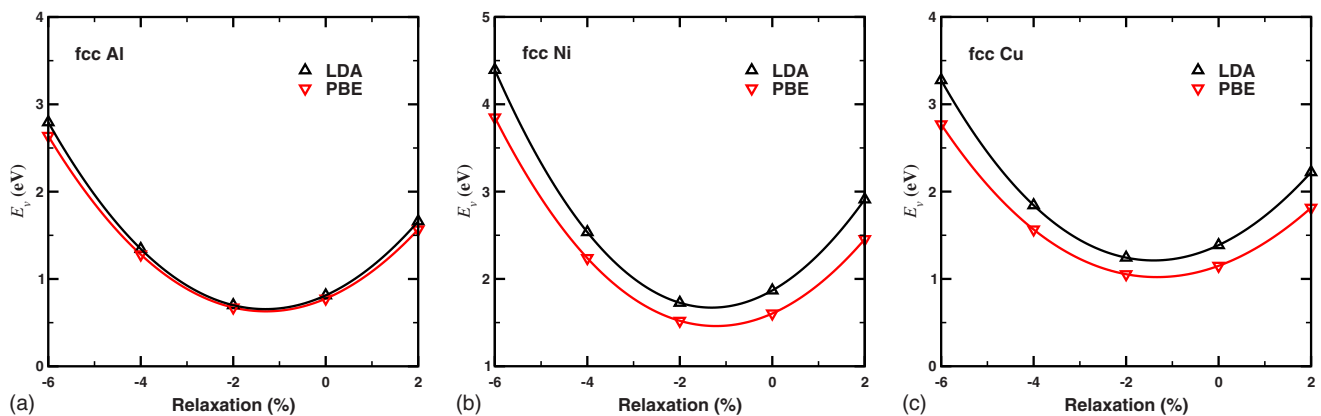
FIG. 1. (Color online) LDA and PBE volume-relaxed vacancy formation energies $[E_v^{32}(\eta)]$ for fcc Al, Ni, and Cu plotted as a function of η describing the local lattice relaxation in the 32-atoms supercells.

TABLE V. Theoretical (EMTO: present results; PP: pseudopotential method, Ref. 8; FPKKR: full-potential Korringa-Kohn-Rostoker method, Ref. 49) and experimental (Ref. 50) vacancy formation energies (in eV) for fcc Al.

	LDA	PBE	PBEsol	AM05	LAG
EMTO	0.65	0.62	0.75	0.89	0.59
PP	0.67	0.61		0.84	0.59
FPKKR	0.66	0.61			
Expt.			0.67 ± 0.03		

the present theoretical vacancy formation energies and the experimental data is 6.7, 18.4, 6.7, 2.2, and 16.8% for LDA, PBE, PBEsol, AM05, and LAG, respectively. It is found that the AM05 functional performs much better for Ni than for Al. At the same time, PBE and LAG only poorly reproduce the recommended experimental vacancy formation energy of Ni. At this point it might be worth pointing out that out of the nine quoted experimental vacancy formation enthalpies for fcc Ni (Ref. 50) only two are close to the recommended value of 1.79 ± 0.05 eV, all the others range between 1.45 and 1.76 eV.

In Table VII, we compare the EMTO results for Cu to those obtained using the linear muffin-tin orbitals (LMTO),[10] the FPKKR,[51] and the full-potential linear muffin-tin orbitals (FPLMTO) (Refs. 52 and 53) methods, as well as to two experimental values.[50,54] The large scatter between the LMTO, FPKKR, and FPLMTO results illustrates the numerical difficulties associated with such calculations and shows the sensitivity of the formation energy to various numerical approximations. All former LDA results from Table VII were obtained for the unrelaxed geometry and thus are expected to overestimate the present LDA value. We note the good agreement between the present unrelaxed value of 1.39 eV (Table III) and that obtained using the FPKKR method.[51]

Finally, we compare the present vacancy formation energy for fcc Cu to the experimental values. Using the recommended experimental value of 1.28 ± 0.05 eV,[50] we might conclude that for Cu the AM05 approximation yields the best performance. However, more recent experiments give 1.19 ± 0.03 eV for the vacancy formation energy in Cu. This value places LDA and PBEsol on the top (error of 1.7%), followed by AM05 (7.6%), LAG (12.6%), and finally PBE (14.3%).

IV. DISCUSSION

A. Volume effect

Before discussing the relative merits of the five functionals, we consider the volume effects in the present E_v values.

For solids the primary and many times the key effect of the exchange-correlation approximation is on the equilibrium volume. For fcc Al, Ni, and Cu, the LDA over-binding (underestimated volume) is efficiently remedied by all gradient-level approximations considered here. One may ask whether the obtained large impact of the exchange-correlation approximations on the theoretical E_v is to some extent related to volume effects. To answer this question, in Fig. 2, we compare the effect of the volume change on the vacancy formation energy of Al, Ni, and Cu to that of the exchange-correlation approximation. The figure displays the EMTO results for E_v (red diamonds) along with five LDA values obtained at the LDA, PBE, PBEsol, AM05, and LAG equilibrium volumes, respectively (black circles). In these additional LDA calculations, both the supercell and the bulk energy was computed at the corresponding gradient-level volumes and the local lattice relaxation was fixed at the equilibrium (LDA) value.

Figure 2 clearly demonstrates the large positive (negative) gradient corrections by AM05 (PBE and LAG) relative to the LDA values. The moderate effect of PBEsol on the LDA vacancy formation energy is evident especially for the transition metals. The calculated LDA-level volume effects are relatively small: E_v changes between 0.03 eV (Al) and 0.09 eV (Ni) when going from the LDA to the PBE volume. These changes can be considered small when compared to the effect of the exchange-correlation approximation. Furthermore, the slight increase in the LDA-level E_v with volume shows no correlation with the effect of the gradient corrections to LDA. Alternatively, repeating the PBE, AM05, and LAG calculations at the LDA volume (not shown) does not significantly alter the large negative (for PBE and LAG) or positive (for AM05) density gradient contributions to E_v. Therefore, our results and conclusions are robust and are expected to remain valid even if the calculations are carried out at specific (e.g., experimental) volumes.

TABLE VI. Theoretical (EMTO: present results; LMTO: linear muffin-tin orbitals method with electrostatic correction, Ref. 10) and experimental (Expt. Ref. 50) vacancy formation energies (in eV) for fcc Ni.

	LDA	PBE	PBEsol	AM05	LAG
EMTO	1.67	1.46	1.67	1.75	1.49
LMTO	1.78[a]				
Expt.			1.79 ± 0.05		

[a]Rigid fcc lattice.

TABLE VII. Theoretical (EMTO: present results; LMTO: linear muffin-tin orbitals method with electrostatic correction, Ref. 10; FPKKR: full-potential Korringa-Kohn-Rostoker method, Ref. 51; FPLMTO: full-potential linear muffin-tin orbitals method, Ref. 52; FPLMTO: full-potential linear muffin-tin orbitals method, Ref. 53) and experimental (Refs. 50 and 54) vacancy formation energies (in eV) for fcc Cu.

	LDA	PBE	PBEsol	AM05	LAG
EMTO	1.21	1.02	1.21	1.28	1.04
LMTO	1.33[e]				
FPKKR	1.41[e]				
FPLMTO[a]	1.29[e]				
FPLMTO[b]	1.33[e]				
Expt.[c]			1.28 ± 0.05		
Expt.[d]			1.19 ± 0.03		

[a]Reference 52.
[b]Reference 53.
[c]Reference 50.
[d]Reference 54.
[e]Rigid fcc lattice.

B. Trends

We have seen that the vacancy formation energies for Al, Ni, and Cu depend very strongly on the involved density functional approximation. It is notable that the theoretical E_v values obtained using different functionals can differ from each other by as much as ~50% (e.g., the AM05 and LAG values from Table V). This large scatter of the theoretical results might indicate that no reliable description of the vacancies in metals is possible within the commonly accepted local- or gradient-level density functional approximations. On the other hand, by monitoring Tables V–VII and Fig. 2, several useful trends can be identified.

All theoretical values are situated between the upper limit given by AM05 and the lower limit set by PBE (except for Al, where LAG gives slightly lower E_v than PBE). On the average, the PBEsol and LDA results are very close to each other (identical for Ni and Cu within the present error bar). Based on the experimental data (Tables V–VII), one concludes that PBE and LAG systematically underestimate whereas AM05 overestimates (except for Ni) the vacancy

formation energy. Introducing mean relative errors for the three fcc metals considered here, we find that LDA, PBE, PBEsol, AM05, and LAG reproduce the experimental vacancy formation enthalpy within 3.8, 13.9, 6.8, 14.2, and 13.8%, respectively. Note that in all cases, LDA yields the best E_v compared to the experiment. On this ground, one may conclude that LDA and PBEsol give the most accurate vacancy formation energies in close-packed metals. We point out that the above conclusion remains valid also within the error bar associated with the employed perturbative approach (see Sec. III A). In such comparisons, however, one should also take into account the accuracy of the functionals in the case of the equation of state. Combining the relative errors for E_v with those obtained for w_0 and B_0 (Table II), for the final errors of LDA, PBE, PBEsol, AM05, and LAG we get 11.4, 7.1, 9.1, 12.2, and 9.5%, respectively. The so defined mean error places PBE and PBEsol on the top followed by LAG, LDA, and AM05.

Before closing this section, we briefly comment on the accuracy of the experimental data for the vacancy formation enthalpy. The quoted experimental values from Tables V–VII
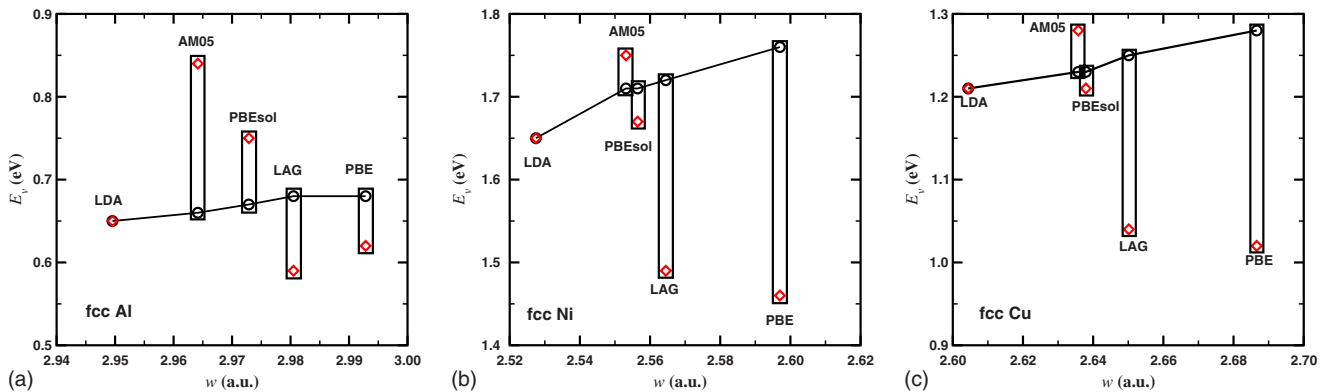
FIG. 2. (Color online) Volume versus exchange-correlation effect in the vacancy formation energy of fcc Al, Ni, and Cu. Red diamonds: self-consistent results from Tables V–VII; black circles: LDA results obtained at the LDA, PBE, PBEsol, AM05, and LAG volumes, respectively. The columns mark the size of the gradient corrections relative to the LDA vacancy formation energies calculated at fixed volume.

are the recommended formation enthalpies from Ref. [50] and they have commonly been used by theoreticians to assess their calculated results.[8,10–16,49,51–53] On the other hand, the actual experimental data from Ref. [50] show a significant scatter around the recommended average values. As we have already pointed out in Sec. III C 2, for fcc Ni the reported experimental enthalpies range between 1.45 and 1.80 eV, whereas for Al (Cu), they vary between 0.60 eV (0.92 eV) and 0.82 eV (1.31 eV). These deviations are on the same order as those between the results obtained with different density functionals. Although more recent experiment for Cu (Ref. [54]) gives somewhat smaller error bar, the large scatter for the measured vacancy formation enthalpies of Al and Ni makes the above performance contrasting strictly valid only with the recommended values.[50] Further accurate experiments are needed before making a more delicate final assessment of the relative merits of the present exchange-correlation approximations for the vacancy formation energies in metals.

C. Vacancies versus close-packed surfaces

It is instructive to contrast the present results for the monovacancies in metals with those obtained for the close-packed surfaces of the late transition metals.[17] Since these two defects have common features (oscillating metallic density and electronic surface) the performances of the density functional approximations are expected to show certain parallelism. According to the previous theoretical study,[17] the surface energies (γ) of the (111) surface of Rh, Pd, and Ag follow the trend $\gamma^{\text{LDA}} > \gamma^{\text{PBEsol}} \gtrsim \gamma^{\text{AM05}} > \gamma^{\text{LAG}} > \gamma^{\text{PBE}}$. The EMTO vacancy formation energies for Ni and Cu satisfy the relation $E_v^{\text{AM05}} > E_v^{\text{LDA}} \approx E_v^{\text{PBEsol}} > E_v^{\text{LAG}} \gtrsim E_v^{\text{PBE}}$, and for Al we have $E_v^{\text{AM05}} > E_v^{\text{PBEsol}} > E_v^{\text{LDA}} > E_v^{\text{PBE}} \gtrsim E_v^{\text{LAG}}$. Thus, for both defects PBE and LAG give the lowest formation energies followed by PBEsol and LDA. AM05 always leads to the largest E_v. Comparing the two recent approximations (PBEsol and AM05), we find that $(E_v^{\text{AM05}} - E_v^{\text{PBEsol}})$ is 0.14 eV for Al, 0.08 eV for Ni, and 0.07 eV for Cu. This finding is quite surprising, since (a) the PBEsol and AM05-level surface energies for late 4d transition metals are close to each other, and (b) both PBEsol and AM05 use the jellium surface data to establish the correlation term. To understand the above behavior, below we examine the differences between the two systems and between the PBEsol and AM05 functionals.

It has been found (Table II and Ref. [17]) that PBEsol and AM05 yield similar equation of states for Al, Ni, and Cu. Hence, we may assume that the observed difference between E_v^{PBEsol} and E_v^{AM05} and the parallelism between γ^{PBEsol} and γ^{AM05} originate from the particular charge distribution around the corresponding defect. Despite the obvious similarities between vacancies and surfaces, there is also a fundamental deviation that deserves some attention. It can most easily be formulated in terms of the two common density parameter: the reduced density gradient defined as $s = |\nabla n|/2(3\pi^2 n)^{1/3} n$ and the electronic Wigner-Seitz radius given by $r_s = (3/4\pi n)^{1/3}$ (n being the electron density). In close-packed metals, when going from the bulk toward the

center of the monovacancy, r_s increases monotonously whereas s first increases, reaches a maximum and then drops to zero around the core of the vacancy (due to the symmetry). Thus, for vacancies the maximum of r_s (i.e., the minimum of the density) corresponds to vanishing reduced density gradient. For metallic surfaces, on the other hand, both r_s and s increase monotonously toward the vacuum. This difference challenges the internal surface approach for vacancies.[14]

Recently, Csonka *et al.*[18] presented a comparison between the spin-unpolarized exchange-correlation enhancement function, $F_{xc}(s, r_s)$, for PBEsol and AM05. They pointed out that the difference between PBEsol and AM05 depends strongly on the s and r_s values. At $s \lesssim 1$, $(F_{xc}^{\text{AM05}}(s, r_s) - F_{xc}^{\text{PBEsol}}(s, r_s)) < 0$ for any r_s, which means that for this regime the absolute value of the AM05 exchange-correlation energy is always smaller than that of PBEsol. Furthermore, for $r_s \gtrsim 2$ and $s \lesssim 0.8$, $(F_{xc}^{\text{AM05}}(s, r_s) - F_{xc}^{\text{PBEsol}}(s, r_s))$ becomes more negative with increasing r_s and s. Finally, for $2 \lesssim r_s \lesssim 5$ the two enhancement functions cross each other at $s \approx 1$ and the positive $(F_{xc}^{\text{AM05}}(s, r_s) - F_{xc}^{\text{PBEsol}}(s, r_s))$ (for $s \gtrsim 1$) increases with increasing s. For more details, see Fig. 2 from Ref. [18].

The characteristic density parameters around the vacancy sites for the present solids are $2 < r_s < 4.7$ and $s < 0.8$ for Al, $1.5 < r_s < 3.7$ and $s < 0.6$ for Ni, and $1.6 < r_s < 3.9$ and $s < 0.7$ for Cu. Therefore, on the average, the Al vacancy possesses the largest r_s (smallest density) and the largest s among the three elements considered here. Taking into account the above-described trend for $(F_{xc}^{\text{AM05}}(s, r_s) - F_{xc}^{\text{PBEsol}}(s, r_s))$, we can easily understand why the total energy for the supercell, and thus the vacancy formation energy, is always larger for AM05 than for PBEsol and why the $(E_v^{\text{AM05}} - E_v^{\text{PBEsol}})$ difference is the largest for Al. Notice that the strong overestimation of the vacancy formation energy by AM05 (especially for Al) originates from the fact that the AM05 enhancement function goes significantly below the PBEsol enhancement function for $s < 0.8$ and large r_s (~ 5). The situation for metallic surfaces is quite different. For this planar defect, r_s and s increase from their bulk values to the infinity. Accordingly, $(F_{xc}^{\text{AM05}}(s, r_s) - F_{xc}^{\text{PBEsol}}(s, r_s))$ scans both the negative (for $s \lesssim 1$ and intermediate r_s) and the positive (for $s \gtrsim 1$ and large r_s) regimes. The corresponding low-s (positive) and large-s (negative) contributions in $(\gamma^{\text{AM05}} - \gamma^{\text{PBEsol}})$ reduce each other to some extent leading to similar surface energies within PBEsol and AM05. We emphasize that an analogous "error" cancellation for vacancies cannot occur because for these defects s is upper bounded and the critical part of the $F_{xc}(s, r_s)$ functions belongs to the $s \lesssim 1$ regime.

V. CONCLUSIONS

Using the exact muffin-tin orbitals method, we have calculated the equation of state and vacancy formation energies for fcc Al, Ni, and Cu. All calculations have been carried out at five different density functional approximation levels: LDA, PBE, PBEsol, AM05, and LAG. We have shown that the numerical error in our vacancy formation energies is

around 0.01 eV. Using former theoretical data, we have demonstrated that the employed theoretical approach is suitable to calculate the vacancy formation energies and to establish the performances of the exchange-correlation approximations for the formation energies of monovacancies in close-packed metals.

We have found that the LDA approximation gives the most accurate vacancy formation energy in Al, Ni, and Cu when compared to the recommended experimental data. Furthermore, on the average, PBE and LAG underestimate whereas AM05 overestimates the vacancy formation energy. At the same time, the PBEsol approximation gives results close to the LDA approximation. Our results for fcc Ni and Cu indicate that the two recent exchange-correlation approximations (PBEsol and AM05) can be used more successfully for the late transition metals than for Al. Starting from the particular charge distribution around metallic monovacancies and surfaces, we have presented a plausible explanation for the observed differences between the results obtained using the PBEsol and AM05 functionals.

Defining the mean error for the vacancy formation energy of Al, Ni, and Cu as the mean difference between the calculated and the recommended experimental values, the LDA and PBEsol turn out to be the most reliable approximation. However, if we also take into account the performances of the functionals for the equation of states, the above verdict is changed in favor of PBE and PBEsol. Nevertheless, one should also keep in mind the large scatter of the actual experimental vacancy formation data around the quoted recommended values, which blurs the above performance-trend to some extent.

The present study is limited to three metals. However, since there is no *a priori* reason for assuming different behavior for the other close-packed metals, the disclosed general trends for the five common exchange-correlation functional can be used to understand and classify future theoretical data for metals and metallic alloys.

ACKNOWLEDGMENTS

[1] P. Hohenberg, and W. Kohn, Phys. Rev. **136**, B864 (1964).

[2] W. Kohn and L. J. Sham, Phys. Rev. **140**, A1133 (1965).

[3] J. P. Perdew, K. Burke, and M. Ernzerhof, Phys. Rev. Lett. **77**, 3865 (1996).

[4] J. P. Perdew, A. Ruzsinszky, G. I. Csonka, O. A. Vydrov, G. E. Scuseria, L. A. Constantin, X. Zhou, and K. Burke, Phys. Rev. Lett. **100**, 136406 (2008). See also the Supplementary Information.

[5] W. Kohn and A. E. Mattsson, Phys. Rev. Lett. **81**, 3487 (1998).

[6] L. Vitos, B. Johansson, J. Kollár, and H. L. Skriver, Phys. Rev. B **62**, 10046 (2000).

[7] L. Vitos, B. Johansson, J. Kollár, and H. L. Skriver, Phys. Rev. A **61**, 052511 (2000).

[8] R. Armiento and A. E. Mattsson, Phys. Rev. B **72**, 085108 (2005).

[9] R. Armiento and A. E. Mattsson, Phys. Rev. B **66**, 165117 (2002).

[10] P. A. Korzhavyi, I. A. Abrikosov, B. Johansson, A. V. Ruban, and H. L. Skriver, Phys. Rev. B **59**, 11693 (1999).

[11] N. Chetty, M. Weinert, T. S. Rahman, and J. W. Davenport, Phys. Rev. B **52**, 6313 (1995).

[12] D. E. Turner, Z. Z. Zhu, C. T. Chan, and K. M. Ho, Phys. Rev. B **55**, 13842 (1997).

[13] T. Hoshino, N. Papanikolaou, R. Zeller, P. H. Dederichs, M. Asato, T. Asada, and N. Stefanou, Comput. Mater. Sci. **14**, 56 (1999).

[14] K. M. Carling, G. Wahnström, T. R. Mattsson, A. E. Mattsson, N. Sandberg, and G. Grimvall, Phys. Rev. Lett. **85**, 3862 (2000).

[15] K. M. Carling, G. Wahnström, T. R. Mattsson, N. Sandberg, and G. Grimvall, Phys. Rev. B **67**, 054101 (2003).

[16] T. Mizuno, M. Asato, T. Hoshino, and K. Kawakami, J. Magn. Magn. Mater. **226-230**, 386 (2001).

[17] M. Ropo, K. Kokko, and L. Vitos, Phys. Rev. B **77**, 195445 (2008).

[18] G. I. Csonka, J. P. Perdew, A. Ruzsinszky, P. H. T. Philipsen, S. Lebegue, J. Paier, O. A. Vydrov, and J. G. Ángyán, Phys. Rev. B **79**, 155107 (2009).

[19] O. K. Andersen, O. Jepsen, and G. Krier, *Lectures on Methods of Electronic Structure Calculations*, edited by V. Kumar, O. K. Andersen, and A. Mookerjee (World Scientific, Singapore, 1994), pp. 63-124.

[20] L. Vitos, H. L. Skriver, B. Johansson, and J. Kollár, Comput. Mater. Sci. **18**, 24 (2000).

[21] L. Vitos, Phys. Rev. B **64**, 014107 (2001).

[22] L. Vitos, *Computational Quantum Mechanics for Materials Engineers* (Springer-Verlag, London, 2007).

[23] M. Zwierzycki and O. K. Andersen, Acta Phys. Pol. A **115**, 64 (2009).

[24] J. Kollár, L. Vitos, and H. L. Skriver, in *Electronic Structure and Physical Properties of Solids: The Uses of the LMTO Method*, Lectures Notes in Physics, edited by H. Dreyssé (Springer-Verlag, Berlin, 2000), p. 85.

[25] L. Vitos, P. A. Korzhavyi, and B. Johansson, Phys. Rev. Lett. **88**, 155501 (2002); Nature Mater. **2**, 25 (2003).

[26] P. Olsson, I. A. Abrikosov, L. Vitos, and J. Wallenius, J. Nucl. Mater. **321**, 84 (2003).

[27] L. Dubrovinsky *et al.*, Nature (London) **422**, 58 (2003).

[28] L. Vitos, P. A. Korzhavyi, and B. Johansson, Phys. Rev. Lett. **96**, 117210 (2006).

[29] N. Dubrovinskaia *et al.*, Phys. Rev. Lett. **95**, 245502 (2005).

[30] A. Taga, L. Vitos, B. Johansson, and G. Grimvall, Phys. Rev. B **71**, 014201 (2005).

[31] L. Huang, L. Vitos, S. K. Kwon, B. Johansson, and R. Ahuja, Phys. Rev. B **73**, 104203 (2006).

[32] J. Zander, R. Sandström, and L. Vitos, Comput. Mater. Sci. **41**, 86 (2007).

[33] A. E. Kissavos, S. I. Simak, P. Olsson, L. Vitos, and I. A. Abrikosov, Comput. Mater. Sci. **35**, 1 (2006).

[34] B. Magyari-Köpe, G. Grimvall, and L. Vitos, Phys. Rev. B **66**, 064210 (2002).

[35] B. Magyari-Köpe, L. Vitos, and G. Grimvall, Phys. Rev. B **70**, 052102 (2004).

[36] B. Magyari-Köpe, L. Vitos, B. Johansson, and J. Kollár, Acta Crystallogr., Sect. B: Struct. Sci. **57**, 491 (2001).

[37] B. Magyari-Köpe, L. Vitos, B. Johansson, and J. Kollár, J. Geophys. Res. **107**, 2136 (2002).

[38] A. Landa, C.-C. Chang, P. N. Kumta, L. Vitos, and I. A. Abrikosov, Solid State Ionics **149**, 209 (2002).

[39] B. Magyari-Köpe, L. Vitos, G. Grimvall, B. Johansson, and J. Kollár, Phys. Rev. B **65**, 193107 (2002).

[40] J. P. Perdew and Y. Wang, Phys. Rev. B **45**, 13244 (1992).

[41] D. M. Ceperley and B. J. Alder, Phys. Rev. Lett. **45**, 566 (1980).

[42] M. Asato, A. Settels, T. Hoshino, T. Asada, S. Blügel, R. Zeller, and P. H. Dederichs, Phys. Rev. B **60**, 5202 (1999).

[43] V. L. Moruzzi, J. F. Janak, and K. Schwarz, Phys. Rev. B **37**, 790 (1988).

[44] D. A. Young, *Phase Diagrams of the Elements* (University of California Press, Berkeley, 1991).

[45] A. E. Mattsson, R. Armiento, J. Paier, G. Kresse, J. M. Wills, and T. R. Mattsson, J. Chem. Phys. **128**, 084714 (2008).

[46] G. Y. Guo and H. H. Wang, Chin. J. Phys. (Taipei) **38**, 949 (2000).

[47] F. D. Murnaghan, Proc. Natl. Acad. Sci. U.S.A. **30**, 244 (1944).

[48] Our test calculations show that the effect of the electronic temperature on the vacancy formation energy of fcc Al is less than 0.01 eV at 500 K. Furthermore, previous molecular dynamics simulations (Ref. 14), accounting for the anharmonic lattice vibrations, demonstrated that the temperature dependence of the vacancy formation enthalpy is negligible up to ~500 K. Therefore, we consider that comparing the present theoretical results obtained for 0 K to the room-temperature experimental data introduces errors that are within the numerical errors of our calculations.

[49] T. Hoshino, M. Asato, R. Zeller, and P. H. Dederichs, Phys. Rev. B **70**, 094118 (2004).

[50] P. Ehrhart, P. Jung, H. Schultz, and H. Ullmaier, in *Atomic Defects in Metals*, edited by H. Ullmaier, Landolt-Börnstein, New Series, Group III, Vol. 25 (Springer-Verlag, Berlin, 1991).

[51] B. Drittler, M. Weinert, R. Zeller, and P. H. Dederichs, Solid State Commun. **79**, 31 (1991).

[52] T. Korhonen, M. J. Puska, and R. M. Nieminen, Phys. Rev. B **51**, 9526 (1995).

[53] H. M. Polatoglou, M. Methfessel, and M. Scheffler, Phys. Rev. B **48**, 1877 (1993).

[54] T. Hehenkamp, W. Berger, J.-E. Kluin, C. Lüdecke, and J. Wolff, Phys. Rev. B **45**, 1998 (1992).